SUPPORTING INFORMATION

FOR

Metabolite Structure Assignment Using *in silico* NMR Techniques.

Susanta Das[a], Arthur S. Edison[b], Kenneth M. Merz, Jr.[a,*]

[a]Department of Chemistry, Michigan State University, 578 S. Shaw Lane, East Lansing, Michigan 48824, USA.

[b]Departments of Genetics and Biochemistry, Institute of Bioinformatics and Complex Carbohydrate Center, University of Georgia, 315 Riverbend Rd, Athens, GA 30602, USA.

[*]E-mail (Kenneth M. Merz, Jr.): merzjrke@msu.edu

Table of Contents

Table S1. Scaling parameters for the ^{1}H and ^{13}C chemical shifts derived from the linear regression method.

Table S2. The relative Gibbs free energy (in kcal mol^{-1}) of each conformer with respect to the most stable structure, Boltzmann distribution of conformers and the Boltzmann mole fraction (in %) for each conformer of L- citrulline.

Table S3. Relative energies, Boltzmann factor and Equilibrium mole fraction of all structurally distinct conformations of O-succinyl-L- homoserine.

Table S4. The relative Gibbs free energy (in kcal mol^{-1}) of each conformer with respect to the most stable structure, Boltzmann distribution of conformers and the Boltzmann mole fraction (in %) for each conformer of 4-hydroxyphenethyl-alcohol.

Table S5. The relative Gibbs free energy (in kcal mol^{-1}) of each conformer with respect to the most stable structure, Boltzmann distribution of conformers and the Boltzmann mole fraction (in %) for each conformer of N-acetyl-D-glucosamine.

Table S6. The relative Gibbs free energy (in kcal mol^{-1}) of each conformer with respect to the most stable structure, Boltzmann distribution of conformers and the Boltzmann mole fraction (in %) for each conformer of N-acetylneuraminic-acid.

Table S7. The relative Gibbs free energy (in kcal mol^{-1}) of each conformer with respect to the most stable structure, Boltzmann distribution of conformers and the Boltzmann mole fraction (in %) for each conformer of Salicylate.

Table S8. The relative Gibbs free energy (in kcal mol^{-1}) of each conformer with respect to the most stable structure, Boltzmann distribution of conformers and the Boltzmann mole fraction (in %) for each conformer of Kanamycin.

Table S9. The relative Gibbs free energy (in kcal mol^{-1}) of each conformer with respect to the most stable structure, Boltzmann distribution of conformers and the Boltzmann mole fraction (in %) for each conformer of Methyl-N-acetyl-alpha-D-glucosaminide.

Table S10. The relative Gibbs free energy (in kcal mol^{-1}) of each conformer with respect to the most stable structure, Boltzmann distribution of conformers and the Boltzmann mole fraction (in %) for each conformer of Pantothenate.

Table S11. The relative Gibbs free energy (in kcal mol^{-1}) of each conformer with respect to the most stable structure, Boltzmann distribution of conformers and the Boltzmann mole fraction (in %) for each conformer of Choline.

Table S12. Computed and experimental ^{1}H NMR chemical shift (in ppm) data of L-citrulline.

Table S13. Computed and experimental ^{13}C NMR chemical shift (in ppm) data of L-citrulline.

Table S14. Computed and available experimental ^{1}H NMR shifts for O-succinyl-L- homoserine.

Table S15. Computed and available experimental ^{13}C NMR chemical shifts for O-succinyl-L- homoserine.

Table S16. Computed and experimental ^{1}H NMR chemical shift (in ppm) data of 4-hydroxyphenethyl-alcohol.

Table S17. Computed and experimental ^{13}C NMR chemical shift (in ppm) data of 4-hydroxyphenethyl-alcohol.

Table S18. Computed and experimental ^{1}H NMR chemical shift (in ppm) data of N-acetyl-D-glucosamine.

Table S19. Computed and experimental ^{13}C NMR chemical shift (in ppm) data of N-acetyl-D-glucosamine.

Table S20. Computed and experimental ^{1}H NMR chemical shift (in ppm) data of N-acetylneuraminic-acid.

Table S21. Computed and experimental ^{13}C NMR chemical shift (in ppm) data of N-acetylneuraminic-acid.

Table S22. Computed and experimental ^{1}H NMR chemical shift (in ppm) data of Salicylate.

Table S23. Computed and experimental ^{13}C NMR chemical shift (in ppm) data of Salicylate.

Table S24. Computed and experimental ^{1}H NMR chemical shift (in ppm) data of Kanamycin.

Table S25. Computed and experimental ^{13}C NMR chemical shift (in ppm) data of Kanamycin.

Table S26. Computed and experimental ^{1}H NMR chemical shift (in ppm) data of Methyl-N-acetyl-alpha-D-glucosaminide.

Table S27. Computed and experimental ^{13}C NMR chemical shift (in ppm) data of Methyl-N-acetyl-alpha-D-glucosaminide.

Table S28. Computed and experimental ^{1}H NMR chemical shift (in ppm) data of Pantothenate.

Table S29. Computed and experimental ^{13}C NMR chemical shift (in ppm) data of Pantothenate.

Table S30. Computed and experimental ^{1}H NMR chemical shift (in ppm) data of Choline.

Table S31. Computed and experimental ^{13}C NMR chemical shift (in ppm) data of Choline.

Table S32. No. of atoms, No. of rotatable bonds, Force-field generated conformation, ANI optimized conformations, and No. of Cluster are reported.

Table S33. Relative energies, Boltzmann factor and Equilibrium mole fraction of all structurally distinct conformations of O-succinyl-L- homoserine (zwitterionic state)

Table S34. The relative Gibbs free energy (in kcal mol^{-1}) of each conformer with respect to the most stable structure, Boltzmann distribution of conformers and the Boltzmann mole fraction (in %) for each conformer of L- citrulline (zwitterionic form).

Table S35. The relative Gibbs free energy (in kcal mol^{-1}) of each conformer with respect to the most stable structure, Boltzmann distribution of conformers and the Boltzmann mole fraction (in %) for each conformer of N-acetylneuraminic-acid (anionic form).

Table S36. Computed and available experimental ^{13}C NMR chemical shifts for O-succinyl-L- homoserine (zwitterionic state)

Table S37. Computed and available experimental ^{13}C NMR chemical shifts for O-succinyl-L- homoserine (zwitterionic state)

Table S38. Computed and experimental ^{1}H NMR chemical shift (in ppm) data of L-citrulline (zwitterionic form)

Table S39. Computed and experimental ^{13}C NMR chemical shift (in ppm) data of L-citrulline (zwitterionic form).

Table S40. Computed and experimental ^{1}H NMR chemical shift (in ppm) data of N-acetylneuraminic-acid (anionic form).

Table S41. Computed and experimental ^{13}C NMR chemical shift (in ppm) data of N-acetylneuraminic-acid (anionic form).

Table S42. Computed and experimental ^{1}H NMR chemical shift (in ppm) data of Salicylate (anionic form).

Table S43. Computed and experimental ^{13}C NMR chemical shift (in ppm) data of Salicylate (anionic form).

Table S44. MAE values of the ^{1}H and ^{13}C NMR chemical shifts.

Figure S1. Plots of the differences between the calculated and experimental ^{1}H and ^{13}C NMR chemical shifts of L- citrulline. Shielding constants were computed at the B3LYP/6311G+(2d, p) level of theory and converted to linear scaled reference chemical shifts. Values of chemical shift differences are given in ppm.

Figure S2. Plots of the differences between the calculated and experimental ^{1}H and ^{13}C NMR chemical shifts of 4-hydroxyphenethyl-alcohol. Shielding constants were computed at the B3LYP/6311G+(2d, p) level of theory and converted to linear scaled reference chemical shifts. Values of chemical shift differences are given in ppm.

Figure S3. Plots of the differences between the calculated and experimental ^{1}H and ^{13}C NMR chemical shifts of N-acetyl-D-glucosamine. Shielding constants were computed at the B3LYP/6311G+(2d, p) level of theory and converted to linear scaled reference chemical shifts. Values of chemical shift differences are given in ppm.

Figure S4. Plots of the differences between the calculated and experimental ^{1}H and ^{13}C NMR chemical shifts of N-acetylneuraminic-acid. Shielding constants were computed at the B3LYP/6311G+(2d, p) level of theory and converted to linear scaled reference chemical shifts. Values of chemical shift differences are given in ppm.

Figure S5. Plots of the differences between the calculated and experimental ^{1}H and ^{13}C NMR chemical shifts of Salicylate. Shielding constants were computed at the B3LYP/6311G+(2d, p) level of theory and converted to linear scaled reference chemical shifts. Values of chemical shift differences are given in ppm.

Figure S6. Plots of the differences between the calculated and experimental ^{1}H and ^{13}C NMR chemical shifts of Kanamycin. Shielding constants were computed at the B3LYP/6311G+(2d, p) level of theory and converted to linear scaled reference chemical shifts. Values of chemical shift differences are given in ppm.

Figure S7. Plots of the differences between the calculated and experimental ^{1}H and ^{13}C NMR chemical shifts of Methyl-N-acetyl-alpha-D-glucosaminide. Shielding constants were computed at the B3LYP/6311G+(2d, p) level of theory and converted to linear scaled reference chemical shifts. Values of chemical shift differences are given in ppm.

Figure S8. Plots of the differences between the calculated and experimental ^{1}H and ^{13}C NMR chemical shifts of Pantothenate. Shielding constants were computed at the B3LYP/6311G+(2d, p) level of theory and converted to linear scaled reference chemical shifts. Values of chemical shift differences are given in ppm.

Figure S9. Plots of the differences between the calculated and experimental ^{1}H and ^{13}C NMR chemical shifts of Choline. Shielding constants were computed at the B3LYP/6311G+(2d, p) level of theory and converted to linear scaled reference chemical shifts. Values of chemical shift differences are given in ppm.

Figure S10. Plots of the differences between the calculated and experimental ^{1}H and ^{13}C NMR chemical shifts of O-succinyl-L-homoserine (zwitterionic form in the solvent, D_2O). Shielding constants were computed at the B3LYP/6311G+(2d, p) level of theory and converted to linear scaled reference chemical shifts. Values of chemical shift differences are given in ppm.

Figure S11. Plots of the differences between the calculated and experimental ^{1}H and ^{13}C NMR chemical shifts of L- citrulline (zwitterionic form). Shielding constants were computed at the B3LYP/6311G+(2d, p) level of theory and converted to linear scaled reference chemical shifts. Values of chemical shift differences are given in ppm.

Figure S12. Plots of the differences between the calculated and experimental ^{1}H and ^{13}C NMR chemical shifts of N-acetylneuraminic-acid (anionic form). Shielding constants were computed at the B3LYP/6311G+(2d, p) level of theory and converted to linear scaled reference chemical shifts. Values of chemical shift differences are given in ppm.

Figure S13. Plots of the differences between the calculated and experimental ^{1}H and ^{13}C NMR chemical shifts of Salicylate (anionic form). Shielding constants were computed at the B3LYP/6311G+(2d, p) level of theory and converted to linear scaled reference chemical shifts. Values of chemical shift differences are given in ppm.

Table S 1. Scaling parameters for the ^{1}H and ^{13}C chemical shifts derived from the linear regression method.

	Scaling factors	
	Slope	Intercept
^{1}H	-1.0767	31.9477
^{13}C	-1.0522	181.2412

Table S 2. The relative Gibbs free energy (in kcal mol^{-1}) of each conformer with respect to the most stable structure, Boltzmann distribution of conformers and the Boltzmann mole fraction (in %) for each conformer of L- citrulline.

Conf. No.	Relative energy (kcal mol^{-1})	Boltzmann factor	Eq. mole fraction (%)
1	1.39	0.095	5.56
2	3.28	0.004	0.23
3	1.07	0.164	9.55
4	1.56	0.072	4.18
5	1.83	0.046	2.66
6	1.87	0.043	2.48
7	1.45	0.087	5.04
8	3.13	0.005	0.30
9	3.36	0.003	0.20
10	1.69	0.058	3.37
11	1.18	0.136	7.89
12	5.59	0.000	0.00
13	0.00	1.000	58.23
14	3.67	0.002	0.12
15	3.43	0.003	0.18

Table S 3. Relative energies, Boltzmann factor and Equilibrium mole fraction of all structurally distinct conformations of O-succinyl-L- homoserine.

Conf. No.	Relative energy (kcal)	Boltzmann factor	Eq. mole fraction (%)
1	1.98	0.035	1.90
2	2.25	0.022	1.21
3	2.88	0.008	0.41
4	3.15	0.005	0.26
5	3.23	0.004	0.23
6	4.93	0.000	0.01
7	4.80	0.000	0.02

8	0.00	1.000	53.84
9	1.21	0.129	6.93
10	2.48	0.015	0.82
11	1.05	0.169	9.08
12	1.93	0.039	2.08
13	3.15	0.005	0.26
14	1.63	0.064	3.45
15	1.22	0.126	6.80
16	3.82	0.002	0.08
17	3.10	0.005	0.29
18	3.31	0.004	0.20
19	2.69	0.011	0.57
20	3.91	0.001	0.07
21	2.14	0.027	1.45
22	1.03	0.175	9.41
23	3.27	0.004	0.21
24	3.69	0.002	0.11
25	3.04	0.006	0.32

Table S 4. The relative Gibbs free energy (in kcal mol^{-1}) of each conformer with respect to the most stable structure, Boltzmann distribution of conformers and the Boltzmann mole fraction (in %) for each conformer of 4-hydroxyphenethyl-alcohol.

Conf. No.	Relative energy (kcal mol^{-1})	Boltzmann factor	Eq. mole fraction (%)
1	0.67	0.324	0.15
2	1.56	0.072	0.03
3	0.43	0.480	0.22
4	0.63	0.345	0.16
5	0.00	1.000	0.45

Table S 5. The relative Gibbs free energy (in kcal mol^{-1}) of each conformer with respect to the most stable structure, Boltzmann distribution of conformers and the Boltzmann mole fraction (in %) for each conformer of N-acetyl-D-glucosamine.

Conf. No.	Relative energy (kcal mol^{-1})	Boltzmann factor	Eq. mole fraction (%)
1	2.48	0.015	0.60
2	2.22	0.023	0.92
3	1.25	0.121	4.76
4	0.14	0.789	31.03
5	1.80	0.048	1.88
6	2.38	0.018	0.70
7	0.66	0.330	12.98
8	1.72	0.054	2.14

9	0.00	1.000	39.35
10	1.15	0.144	5.65

Table S 6. The relative Gibbs free energy (in kcal mol^{-1}) of each conformer with respect to the most stable structure, Boltzmann distribution of conformers and the Boltzmann mole fraction (in %) for each conformer of N-acetylneuraminic-acid.

Conf. No.	Relative energy (kcal mol^{-1})	Boltzmann factor	Eq. mole fraction (%)
1	4.76	0.000	0.02
2	5.56	0.000	0.01
3	4.98	0.000	0.01
4	2.50	0.015	0.98
5	2.37	0.018	1.22
6	4.00	0.001	0.08
7	2.90	0.007	0.50
8	3.62	0.002	0.15
9	3.15	0.005	0.33
10	4.03	0.001	0.07
11	2.38	0.018	1.19
12	4.62	0.000	0.03
13	4.57	0.000	0.03
14	5.17	0.000	0.01
15	1.66	0.060	4.02
16	3.96	0.001	0.08
17	0.00	1.000	66.73
18	0.60	0.362	24.14
19	3.04	0.006	0.39
20	6.90	0.000	0.00

Table S 7. The relative Gibbs free energy (in kcal mol^{-1}) of each conformer with respect to the most stable structure, Boltzmann distribution of conformers and the Boltzmann mole fraction (in %) for each conformer of Salicylate.

Conf. No.	Relative energy (kcal mol^{-1})	Boltzmann factor	Eq. mole fraction (%)
1	0.34	0.566	36.16
2	0.00	1.000	63.84

Table S 8. The relative Gibbs free energy (in kcal mol^{-1}) of each conformer with respect to the most stable structure, Boltzmann distribution of conformers and the Boltzmann mole fraction (in %) for each conformer of Kanamycin.

Conf. No.	Relative energy (kcal mol^{-1})	Boltzmann factor	Eq. mole fraction (%)
1	1.98	0.035	1.90
2	2.25	0.022	1.21
3	2.88	0.008	0.41
4	3.15	0.005	0.26
5	3.23	0.004	0.23

6	4.93	0.000	0.01
7	4.80	0.000	0.02
8	0.00	1.000	53.84
9	1.21	0.129	6.93
10	2.48	0.015	0.82
11	1.05	0.169	9.08
12	1.93	0.039	2.08
13	3.15	0.005	0.26
14	1.63	0.064	3.45
15	1.22	0.126	6.80
16	3.82	0.002	0.08
17	3.10	0.005	0.29
18	3.31	0.004	0.20
19	2.69	0.011	0.57
20	3.91	0.001	0.07

Table S 9. The relative Gibbs free energy (in kcal mol^{-1}) of each conformer with respect to the most stable structure, Boltzmann distribution of conformers and the Boltzmann mole fraction (in %) for each conformer of Methyl-N-acetyl-alpha-D-glucosaminide.

Conf. No.	Relative energy (kcal mol^{-1})	Boltzmann factor	Eq. mole fraction (%)
1	6.84	0.000	0.00
2	5.75	0.000	0.00
3	0.00	1.000	0.54
4	3.83	0.002	0.00
5	0.21	0.697	0.38
6	6.64	0.000	0.00
7	6.63	0.000	0.00
8	5.45	0.000	0.00
9	1.09	0.157	0.08
10	8.36	0.000	0.00

Table S 10. The relative Gibbs free energy (in kcal mol^{-1}) of each conformer with respect to the most stable structure, Boltzmann distribution of conformers and the Boltzmann mole fraction (in %) for each conformer of Pantothenate.

Conf. No.	Relative energy (kcal mol^{-1})	Boltzmann factor	Eq. mole fraction (%)
1	5.49	0.000	0.00
2	0.30	0.598	0.21
3	0.00	1.000	0.36
4	3.43	0.003	0.00
5	1.56	0.072	0.03
6	4.48	0.001	0.00
7	2.11	0.028	0.01
8	4.26	0.001	0.00
9	0.76	0.277	0.10
10	5.08	0.000	0.00
11	0.62	0.348	0.12
12	2.21	0.024	0.01

13	2.52	0.014	0.01
14	10.75	0.000	0.00
15	0.99	0.188	0.07
16	2.74	0.010	0.00
17	3.83	0.002	0.00
18	2.66	0.011	0.00
19	3.75	0.002	0.00
20	3.77	0.002	0.00
21	3.84	0.002	0.00
22	7.75	0.000	0.00
23	1.07	0.163	0.06
24	1.93	0.038	0.01
25	2.50	0.015	0.01

Table S 11. The relative Gibbs free energy (in kcal mol^{-1}) of each conformer with respect to the most stable structure, Boltzmann distribution of conformers and the Boltzmann mole fraction (in %) for each conformer of Choline.

Conf. No.	Relative energy (kcal mol^{-1})	Boltzmann factor	Eq. mole fraction (%)
1	0.69	0.313	12.09
2	0.00	1.000	38.56
3	2.17	0.026	0.99
4	2.61	0.012	0.47
5	0.06	0.897	34.61
6	0.65	0.333	12.85
7	2.64	0.011	0.44

Table S 12. Computed and experimental ^{1}H NMR chemical shift (in ppm) data of L-citrulline.

Atom No.	Chemical Shift (ppm)	Exp. Chemical Shift (ppm)
H25	6.737	
H19	3.669	3.743
H20	1.560	
H21	1.891	
H15	1.682	1.865
H16	2.124	1.865
H13	1.429	1.559
H14	1.595	1.559
H17	3.090	3.134
H18	2.889	3.134
H24	6.833	
H22	3.766	
H23	4.067	

Table S 13. Computed and experimental ^{13}C NMR chemical shift (in ppm) data of L-citrulline.

Atom No.	Chemical Shift (ppm)	Exp. Chemical Shift (ppm)

C5	177.285	177.428
C4	52.457	57.203
C2	33.578	30.459
C1	22.159	27.680
C3	39.875	41.913
C6	156.537	164.305

Table S 14. Computed and available experimental ^{1}H NMR shifts for O-succinyl-L- homoserine.

Atom No.	Chemical Shift (ppm)	Exp. Chemical Shift (ppm)
H16	2.739	2.611
H17	2.710	2.469
H18	2.738	2.611
H19	2.664	2.469
H20	2.135	2.240
H21	1.827	2.240
H22	3.994	4.262
H23	4.219	4.262
H24	3.606	3.842
H25	1.373	-
H26	1.237	-
H27	6.638	-
H28	6.942	-

Table S 15. Computed and available experimental ^{13}C NMR chemical shifts for O-succinyl-L- homoserine.

Atom No.	Chemical Shift (ppm)	Exp. Chemical Shift (ppm)
C1	30.039	33.200
C2	31.209	34.644
C3	33.214	32.044
C4	63.174	64.459
C5	52.461	55.519
C6	173.748	-
C7	172.761	-
C8	177.029	-

Table S 16. Computed and experimental ^{1}H NMR chemical shift (in ppm) data of 4-hydroxyphenethyl-alcohol.

Atom No.	Chemical Shift (ppm)	Exp. Chemical Shift (ppm)
H11	7.078	7.177
H12	7.174	7.177
H13	6.704	6.859
H14	6.750	6.859
H15	2.707	2.775
H16	2.743	2.775
H17	3.784	3.778
H18	3.788	3.778
H19	1.200	
H20	4.855	

Table S 17. Computed and experimental ^{13}C NMR chemical shift (in ppm) data of 4-hydroxyphenethyl-alcohol.

Atom No.	Chemical Shift (ppm)	Exp. Chemical Shift (ppm)
C1	128.571	133.011
C2	127.024	133.011
C3	110.595	118.097
C4	111.288	118.097
C5	38.025	39.605
C6	64.475	65.463
C7	130.974	133.653
C8	152.984	156.523

Table S 18. Computed and experimental ^{1}H NMR chemical shift (in ppm) data of N-acetyl-D-glucosamine.

Atom No.	Chemical Shift (ppm)	Exp. Chemical Shift (ppm)
H16	1.858	2.043
H17	2.016	2.043
H18	1.972	2.043
H19	3.857	3.829
H20	3.836	3.816
H21	3.434	3.845
H22	3.593	3.869
H23	3.612	3.481
H24	3.559	3.760
H25	4.905	5.191
H26	5.918	
H27	1.773	
H28	2.870	
H29	3.456	
H30	3.062	

Table S 19. Computed and experimental ^{13}C NMR chemical shift (in ppm) data of N-acetyl-D-glucosamine.

Atom No.	Chemical Shift (ppm)	Exp. Chemical Shift (ppm)
C1	21.090	24.888
C2	62.791	63.426
C3	171.429	177.490
C4	73.106	78.660

C5	56.011	59.382
C6	72.489	72.750
C7	76.390	76.593
C8	93.785	97.635

Table S 20. Computed and experimental ^{1}H NMR chemical shift (in ppm) data of N-acetylneuraminic-acid.

Atom No.	Chemical Shift (ppm)	Exp. Chemical Shift (ppm)
H22	1.993	2.045
H23	2.393	2.045
H24	1.755	2.045
H25	2.218	2.009
H26	2.079	2.009
H27	3.575	3.718
H28	3.989	3.718
H29	3.783	4.019
H30	3.716	3.752
H31	3.699	3.903
H32	3.705	3.503
H33	3.864	3.978
H34	5.590	
H35	1.496	
H36	1.345	
H37	2.583	
H38	2.966	
H39	6.931	
H40	3.185	

Table S 21. Computed and experimental ^{13}C NMR chemical shift (in ppm) data of N-acetylneuraminic-acid.

Atom No.	Chemical Shift (ppm)	Exp. Chemical Shift (ppm)
C1	22.046	24.819
C2	38.029	42.090
C3	64.183	66.006
C4	170.672	
C5	69.101	70.005
C6	70.019	73.015
C7	51.839	54.968
C8	73.494	71.251
C9	73.164	72.909
C10	167.818	
C11	93.926	99.105

Table S 22. Computed and experimental ^{1}H NMR chemical shift (in ppm) data of Salicylate.

Atom No.	Chemical Shift (ppm)	Exp. Chemical Shift (ppm)
H11	6.939	6.952

H12	7.521	7.451
H13	7.667	7.818
H14	6.958	6.952
H15	8.907	
H16	8.870	

Table S 23. Computed and experimental ^{13}C NMR chemical shift (in ppm) data of Salicylate.

Atom No.	Chemical Shift (ppm)	Exp. Chemical Shift (ppm)
C1	117.174	122.098
C2	134.950	136.705
C3	127.875	133.200
C4	115.008	119.007
C5	109.821	120.713
C6	158.376	162.310
C7	166.471	

Table S 24. Computed and experimental ^{1}H NMR chemical shift (in ppm) data of Kanamycin.

Atom No.	Chemical Shift (ppm)	Exp. Chemical Shift (ppm)
H34	2.194	2.393
H35	1.909	1.798
H36	3.619	3.457
H37	3.113	3.155
H38	3.202	3.810
H39	3.191	3.810
H40	3.601	3.765
H41	3.117	3.431
H42	3.709	4.012
H43	4.101	3.929
H44	3.755	3.686
H45	3.618	3.460
H46	3.064	3.365
H47	3.718	3.954
H48	3.730	3.780
H49	3.503	3.660
H50	3.933	3.895
H51	3.321	3.702
H52	3.903	3.787
H53	4.611	5.146
H54	5.134	5.609
H55	4.091	
H56	2.409	
H57	0.091	
H58	5.403	
H59	5.111	
H60	2.302	
H61	0.493	
H62	0.234	
H63	3.678	
H64	3.098	

H65	3.710	
H66	2.703	
H67	0.455	
H68	2.495	
H69	1.674	

Table S 25. Computed and experimental ^{13}C NMR chemical shift (in ppm) data of Kanamycin.

Atom No.	Chemical Shift (ppm)	Exp. Chemical Shift (ppm)
C1	33.549	32.427
C2	44.819	43.202
C3	61.502	62.596
C4	49.101	50.886
C5	50.713	52.838
C6	69.908	71.349
C7	69.519	71.237
C8	70.904	68.491
C9	56.810	57.712
C10	71.501	73.843
C11	74.920	75.297
C12	72.185	74.826
C13	75.073	73.736
C14	75.709	76.150
C15	85.198	87.470
C16	82.093	82.376
C17	101.901	103.106
C18	97.163	99.391

Table S 26. Computed and experimental ^{1}H NMR chemical shift (in ppm) data of Methyl-N-acetyl-alpha-D-glucosaminide.

Atom No.	Chemical Shift (ppm)	Exp. Chemical Shift (ppm)
H17	2.444	2.028
H18	1.583	2.028
H19	2.499	2.028
H20	3.429	3.376
H21	3.059	3.376
H22	3.662	3.376
H23	4.434	3.732
H24	3.618	3.732
H25	3.833	3.469
H26	3.461	4.751
H27	3.615	3.732
H28	4.180	3.897
H29	4.702	3.897
H30	5.993	
H31	1.233	
H32	1.978	
H33	2.299	

Table S 27. Computed and experimental ^{13}C NMR chemical shift (in ppm) data of Methyl-N-acetyl-alpha-D-glucosaminide.

Atom No.	Chemical Shift (ppm)	Exp. Chemical Shift (ppm)
C1	21.213	24.595
C2	52.026	57.842
C3	62.241	63.243
C4	172.736	177.781
C5	75.657	72.662
C6	55.186	56.329
C7	70.087	73.817
C8	70.944	74.368
C9	95.534	100.785

Table S 28. Computed and experimental ^{1}H NMR chemical shift (in ppm) data of Pantothenate.

Atom No.	Chemical Shift (ppm)	Exp. Chemical Shift (ppm)
H16	1.037	0.919
H17	0.648	0.919
H18	1.044	0.919
H19	0.992	0.919
H20	0.653	0.919
H21	1.263	0.919
H22	2.911	3.429
H23	2.472	3.429
H24	3.701	3.429
H25	3.163	3.429
H26	3.599	3.429
H27	3.613	3.429
H28	4.052	3.971
H29	6.674	
H30	2.197	
H31	7.398	
H32	3.738	

Table S 29. Computed and experimental ^{13}C NMR chemical shift (in ppm) data of Pantothenate.

Atom No.	Chemical Shift (ppm)	Exp. Chemical Shift (ppm)
C1	19.214	23.234
C2	18.506	23.234
C3	34.832	39.377
C4	36.262	39.377
C5	70.946	71.100
C6	172.776	177.649
C7	76.584	78.459
C8	172.038	183.020
C9	39.650	41.277

Table S 30. Computed and experimental ^{1}H NMR chemical shift (in ppm) data of Choline.

Atom No.	Chemical Shift (ppm)	Exp. Chemical Shift (ppm)
H8	2.890	3.195
H9	2.986	3.195
H10	2.845	3.195
H11	2.827	3.195
H12	3.311	3.195
H13	3.165	3.195
H14	2.815	3.195
H15	2.838	3.195
H16	3.395	3.195
H17	3.320	3.514
H18	3.101	3.514
H19	3.947	4.053
H20	4.157	4.053
H21	1.640	

Table S 31. Computed and experimental ^{13}C NMR chemical shift (in ppm) data of Choline.

Atom No.	Chemical Shift (ppm)	Exp. Chemical Shift (ppm)
C1	51.376	56.615
C2	50.365	56.615
C3	53.361	56.615
C4	64.986	70.141
C5	57.822	58.325

Table S 32. No. of atoms, No. of rotatable bonds, Force-field generated conformation, ANI optimized conformations, and No. of Cluster are reported.

No	Metabolites (ionic form)	No. of atoms	No. of rotatable bonds	Conf. Nos. (FF)	ANI Optimized Conf. Nos.	Number of clusters
1	L- citrulline	25	6	107	107	12
2	O-succinyl-L-homoserine	27	8	42	42	5
3	N-acetylneuraminic-acid	39	10	85	85	9
4	Salicylate	15	1	1	1	-

Table S 33. Relative energies, Boltzmann factor and Equilibrium mole fraction of all structurally distinct conformations of O-succinyl-L- homoserine (zwitterionic state)

Conf No.	Relative energy (kcal)	Boltzmann factor	Eq. mole fraction (%)
1	1.59	0.07	4.73
2	0.00	1.00	69.63
3	2.40	0.02	1.22

4	3.88	0.00	0.10
5	0.62	0.35	24.32

Table S 34. The relative Gibbs free energy (in kcal mol^{-1}) of each conformer with respect to the most stable structure, Boltzmann distribution of conformers and the Boltzmann mole fraction (in %) for each conformer of L- citrulline (zwitterionic form).

Conf. No.	Relative energy (kcal mol^{-1})	Boltzmann factor	Eq. mole fraction (%)
1	3.87	0.001	0.00
2	2.51	0.014	0.01
3	1.55	0.073	0.04
4	2.84	0.008	0.00
5	2.62	0.012	0.01
6	0.00	1.000	0.59
7	0.72	0.299	0.18
8	2.48	0.015	0.01
9	3.52	0.003	0.00
10	2.98	0.007	0.00
11	0.98	0.190	0.11
12	1.54	0.074	0.04

Table S 35. The relative Gibbs free energy (in kcal mol^{-1}) of each conformer with respect to the most stable structure, Boltzmann distribution of conformers and the Boltzmann mole fraction (in %) for each conformer of N-acetylneuraminic-acid (anionic form).

Conf. No.	Relative energy (kcal mol^{-1})	Boltzmann factor	Eq. mole fraction (%)
1	1.91	0.040	0.03
2	1.35	0.101	0.07

3	1.77	0.051	0.03
4	1.80	0.048	0.03
5	1.43	0.090	0.06
6	4.45	0.001	0.00
7	1.30	0.111	0.08
8	2.94	0.007	0.00
9	0.00	1.000	0.69

Table S 36. Computed and available experimental ^{13}C NMR chemical shifts for O-succinyl-L- homoserine (zwitterionic state)

Atom	Computed	Experimental
H16	2.277	2.611
H17	2.327	2.469
H18	2.543	2.611
H19	2.498	2.469
H20	2.179	2.240
H21	2.400	2.240
H22	3.857	4.262
H23	4.017	4.262
H24	3.624	3.842
H25	6.548	
H26	10.562	
H27	4.840	

Table S 37. Computed and available experimental ^{13}C NMR chemical shifts for O-succinyl-L- homoserine (zwitterionic state)

Atom	Computed	Experimental
C1	38.203	33.200
C2	34.991	34.644
C3	29.396	32.044
C4	62.805	64.459
C5	55.851	55.519
C6	179.992	
C7	175.638	
C8	169.767	

Table S 38. Computed and experimental ^{1}H NMR chemical shift (in ppm) data of L-citrulline (zwitterionic form)

Atom No.	Chemical Shift (ppm)	Exp. Chemical Shift (ppm)
H13	1.608	1.559
H14	1.609	1.559
H15	1.858	1.865
H16	2.009	1.865
H17	2.908	3.134
H18	3.221	3.134
H19	3.690	3.743
H20	5.133	
H21	4.385	
H22	4.058	
H23	3.930	
H24	4.588	

H25	4.451	

Table S 39. Computed and experimental ^{13}C NMR chemical shift (in ppm) data of L-citrulline (zwitterionic form).

Atom No.	Chemical Shift (ppm)	Exp. Chemical Shift (ppm)
C1	24.906	27.680
C2	30.806	30.459
C3	39.939	41.913
C4	55.190	57.203
C5	170.442	177.428
C6	156.656	164.305

Table S 40. Computed and experimental ^{1}H NMR chemical shift (in ppm) data of N-acetylneuraminic-acid (anionic form).

Atom No.	Chemical Shift (ppm)	Exp. Chemical Shift (ppm)
H22	2.003	2.045
H23	1.826	2.045
H24	1.949	2.045
H25	1.915	2.009
H26	2.062	2.009
H27	3.410	3.718
H28	4.026	3.718
H29	3.685	4.019
H30	3.835	3.752
H31	3.914	3.903
H32	3.608	3.503
H33	4.336	3.978
H34	6.087	
H35	1.483	
H36	8.076	
H37	3.043	

H38	2.569	
H39	4.691	

Table S 41. Computed and experimental ^{13}C NMR chemical shift (in ppm) data of N-acetylneuraminic-acid (anionic form).

Atom No.	Chemical Shift (ppm)	Exp. Chemical Shift (ppm)
C1	21.666	24.819
C2	33.615	42.090
C3	63.605	66.006
C4	168.957	
C5	66.948	70.005
C6	72.429	73.015
C7	48.622	54.968
C8	71.862	71.251
C9	69.980	72.909
C10	171.771	
C11	93.939	99.105

Table S 42. Computed and experimental ^{1}H NMR chemical shift (in ppm) data of Salicylate (anionic form).

Atom No.	Chemical Shift (ppm)	Exp. Chemical Shift (ppm)
H11	6.701	6.952
H12	7.240	7.451
H13	7.787	7.818
H14	6.761	6.952
H15	14.851	

Table S 43. Computed and experimental ^{13}C NMR chemical shift (in ppm) data of Salicylate (anionic form).

Atom No.	Chemical Shift (ppm)	Exp. Chemical Shift (ppm)
C1	113.868	122.098
C2	130.172	136.705
C3	127.698	133.200
C4	113.043	119.007
C5	116.841	120.713
C6	160.696	162.310
C7	171.400	178.336

Table S 44. MAE values of the ^{1}H and ^{13}C NMR chemical shifts. Values are in ppm unit.

No.	**Metabolite (Ionic state in the solvent, D_2O)**	**MAE**	
		^{1}H	**^{13}C**
1	O-succinyl-L-homoserine	0.185	1.997
2	L- citrulline	0.088	3.624
3	N-acetylneuraminic-acid	0.167	3.636
4	Salicylate	0.171	4.379

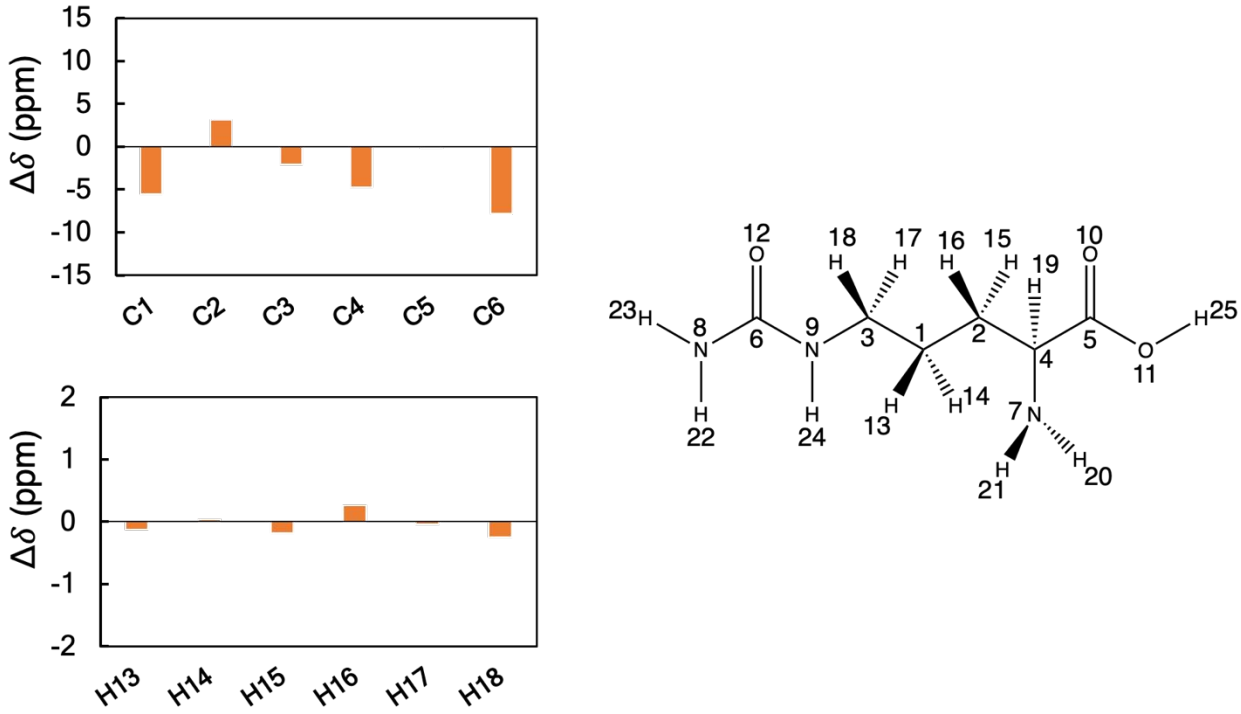

Figure S1. Plots of the differences between the calculated and experimental ^{1}H and ^{13}C NMR chemical shifts of L- citrulline. Shielding constants were computed at the B3LYP/6311G+(2d, p) level of theory and converted to linear scaled reference chemical shifts. Values of chemical shift differences are given in ppm.

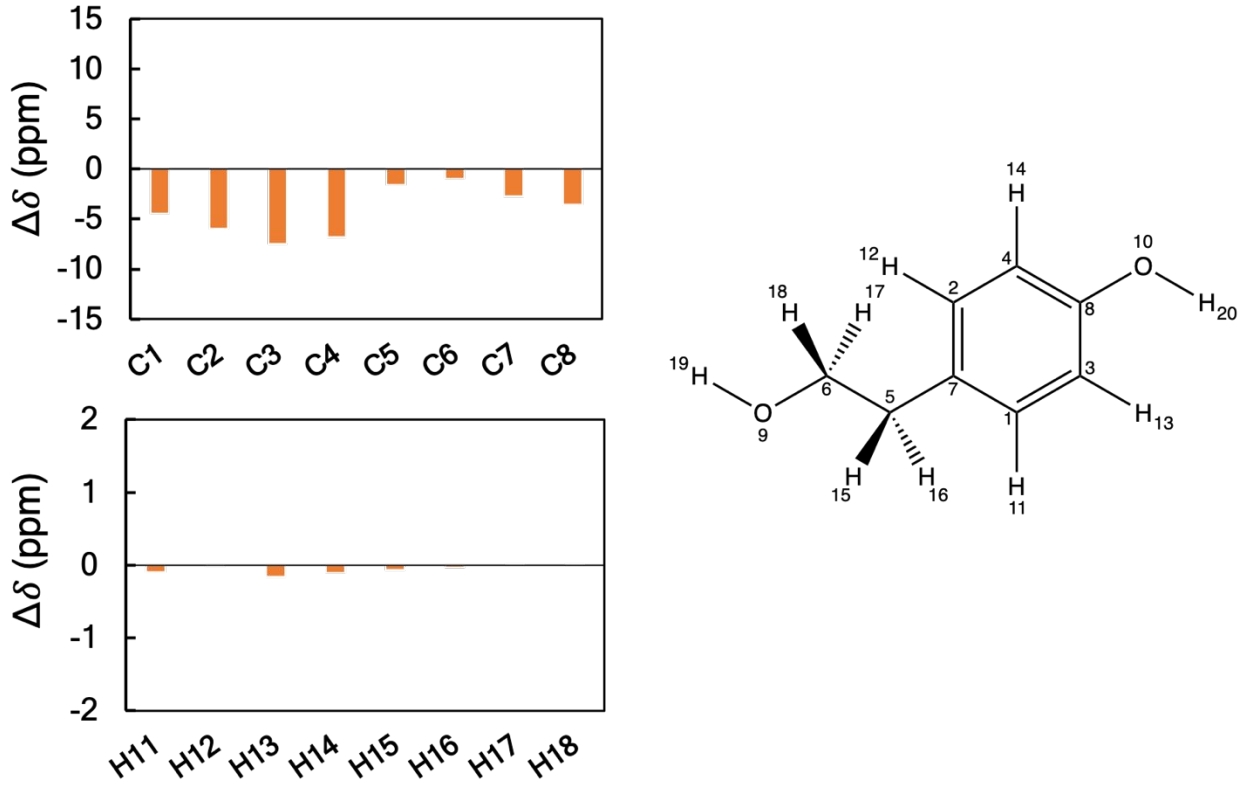

Figure S2. Plots of the differences between the calculated and experimental ^{1}H and ^{13}C NMR chemical shifts of 4-hydroxyphenethyl-alcohol. Shielding constants were computed at the B3LYP/6311G+(2d, p) level of theory and converted to linear scaled reference chemical shifts. Values of chemical shift differences are given in ppm.

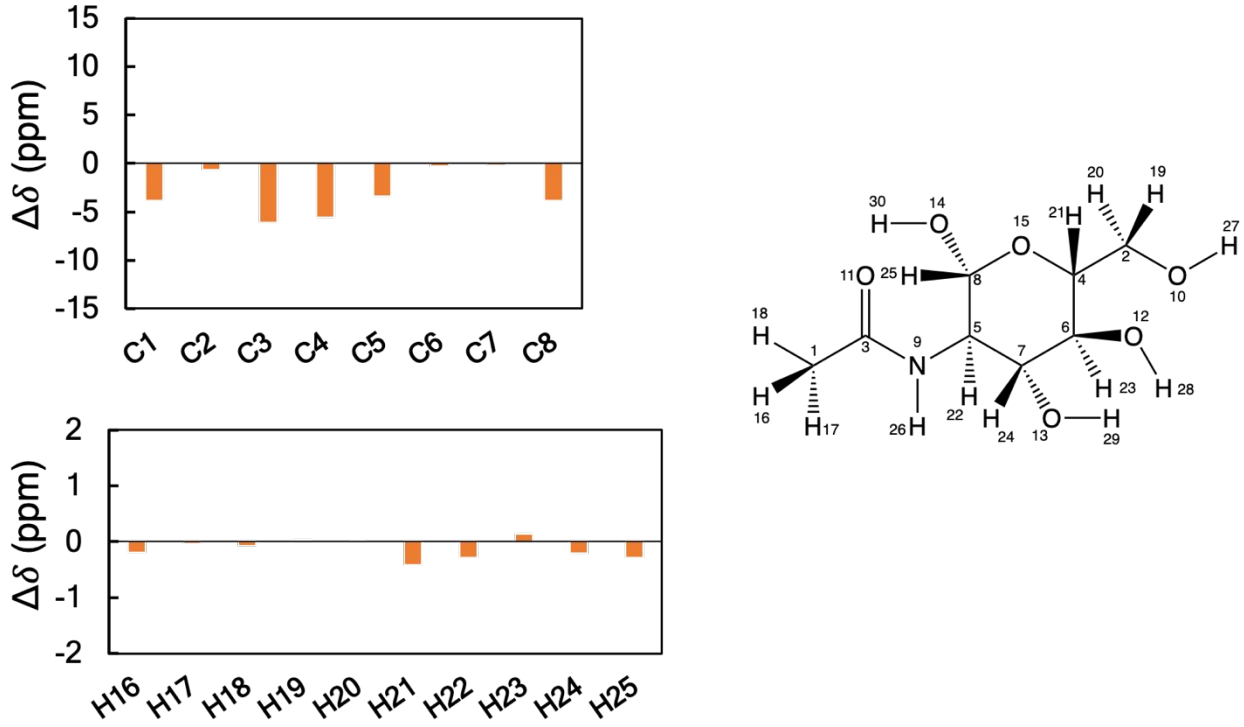

Figure S3. Plots of the differences between the calculated and experimental ^{1}H and ^{13}C NMR chemical shifts of N-acetyl-D-glucosamine. Shielding constants were computed at the B3LYP/6311G+(2d, p) level of theory and converted to linear scaled reference chemical shifts. Values of chemical shift differences are given in ppm.

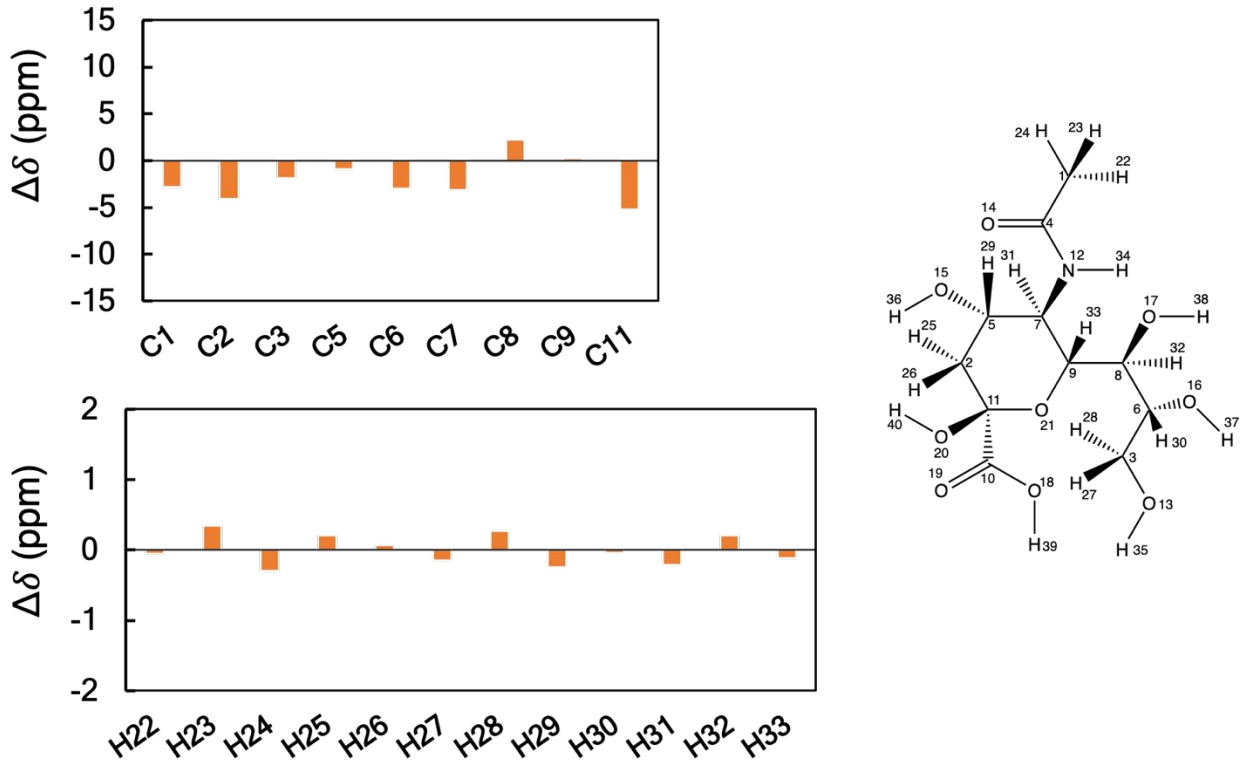

Figure S4. Plots of the differences between the calculated and experimental ^{1}H and ^{13}C NMR chemical shifts of N-acetylneuraminic-acid. Shielding constants were computed at the B3LYP/6311G+(2d, p) level of theory and converted to linear scaled reference chemical shifts. Values of chemical shift differences are given in ppm.

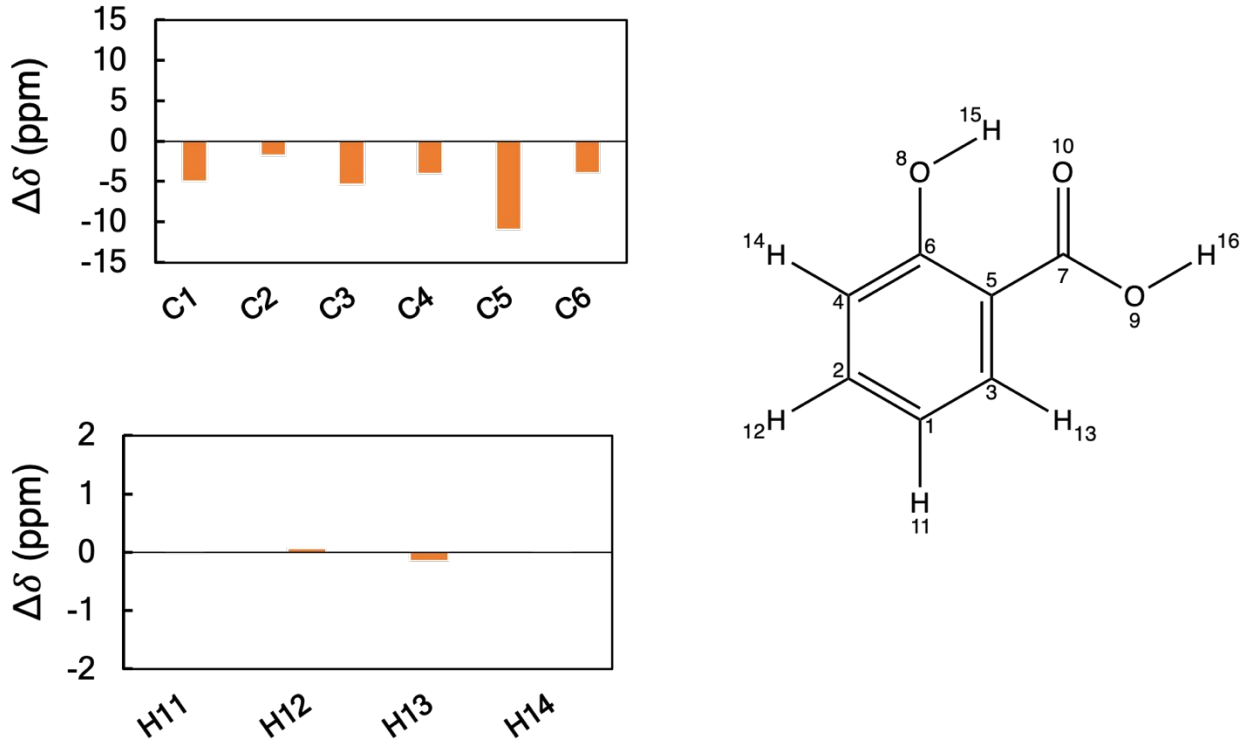

Figure S5. Plots of the differences between the calculated and experimental ^{1}H and ^{13}C NMR chemical shifts of Salicylate. Shielding constants were computed at the B3LYP/6311G+(2d, p) level of theory and converted to linear scaled reference chemical shifts. Values of chemical shift differences are given in ppm.

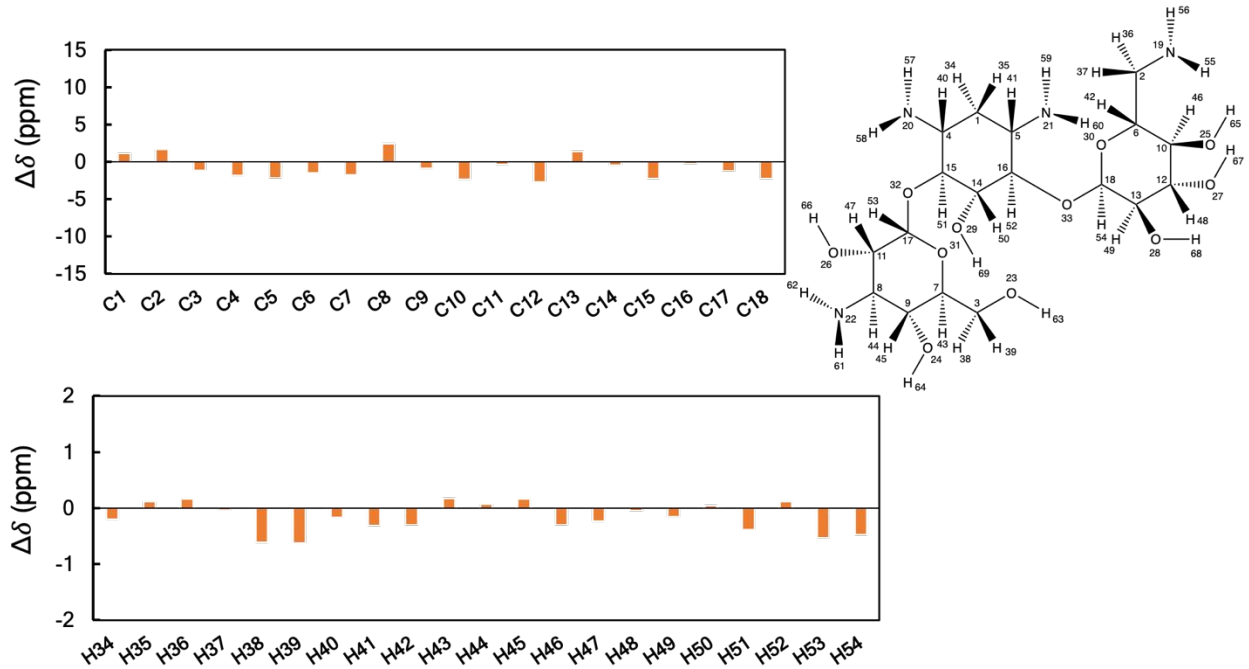

Figure S6. Plots of the differences between the calculated and experimental ^{1}H and ^{13}C NMR chemical shifts of Kanamycin. Shielding constants were computed at the B3LYP/6311G+(2d, p) level of theory and converted to linear scaled reference chemical shifts. Values of chemical shift differences are given in ppm.

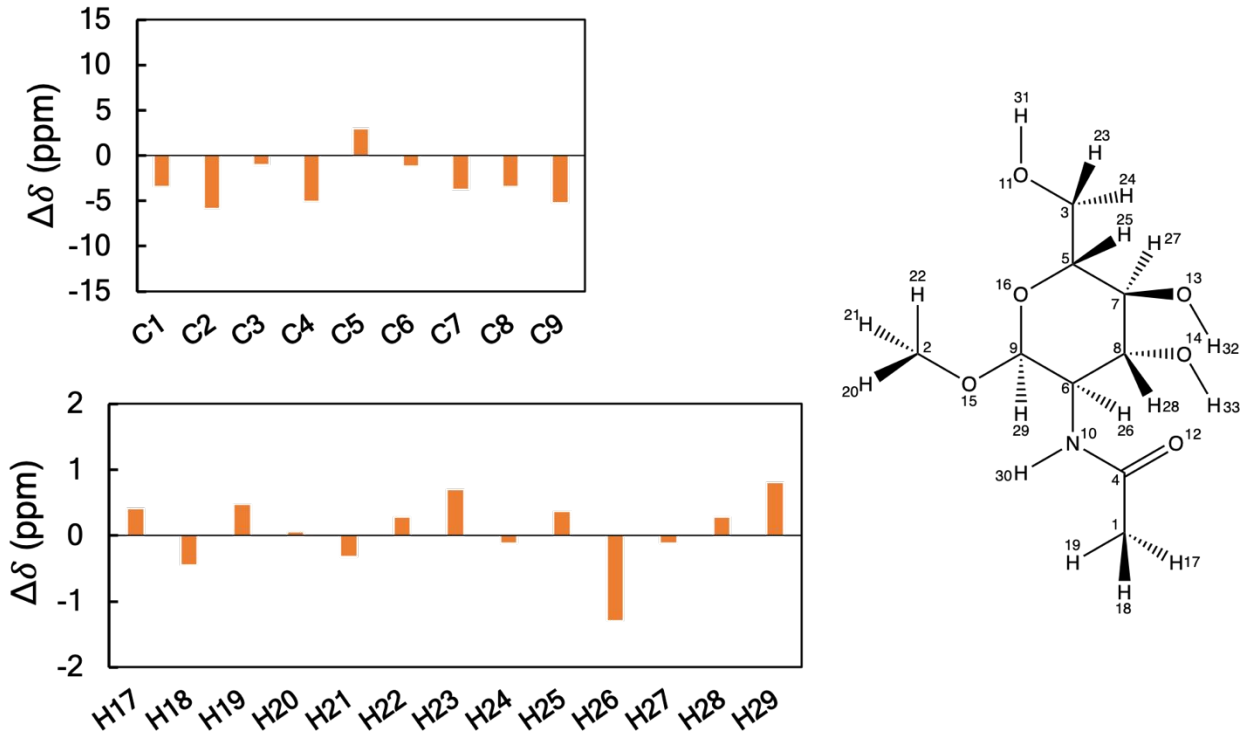

Figure S7. Plots of the differences between the calculated and experimental ^{1}H and ^{13}C NMR chemical shifts of Methyl-N-acetyl-alpha-D-glucosaminide. Shielding constants were computed at the B3LYP/6311G+(2d, p) level of theory and converted to linear scaled reference chemical shifts. Values of chemical shift differences are given in ppm.

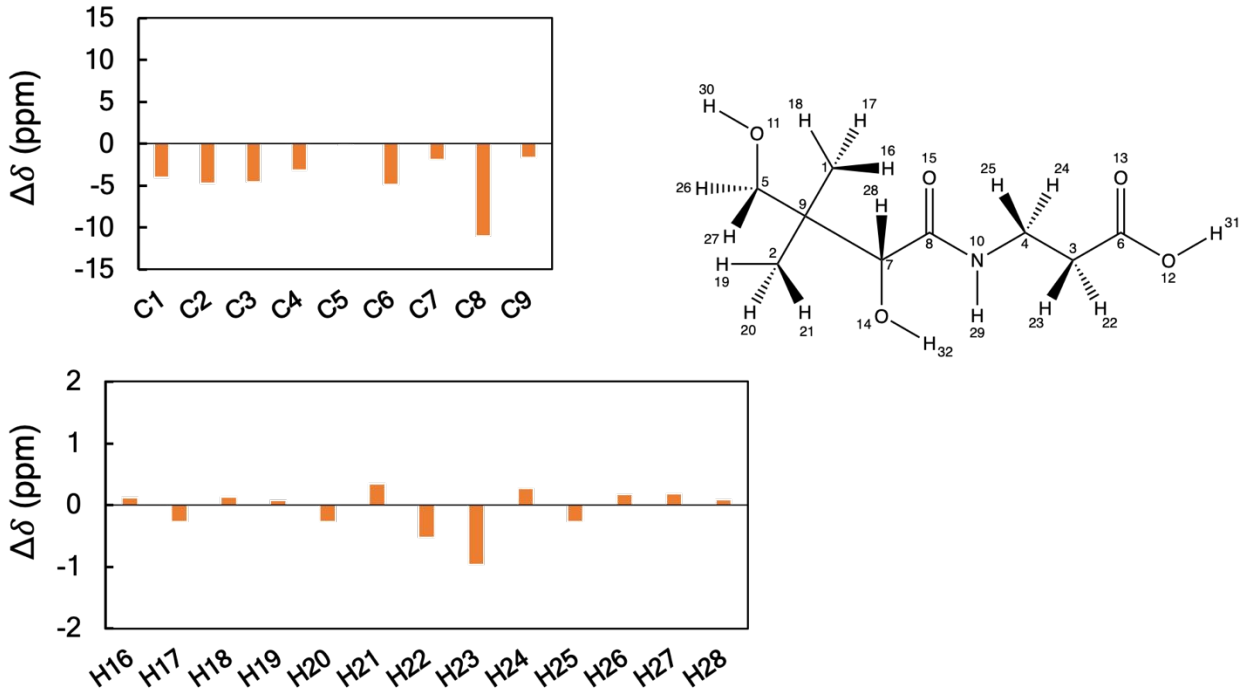

Figure S8. Plots of the differences between the calculated and experimental ^{1}H and ^{13}C NMR chemical shifts of Pantothenate. Shielding constants were computed at the B3LYP/6311G+(2d, p) level of theory and converted to linear scaled reference chemical shifts. Values of chemical shift differences are given in ppm.

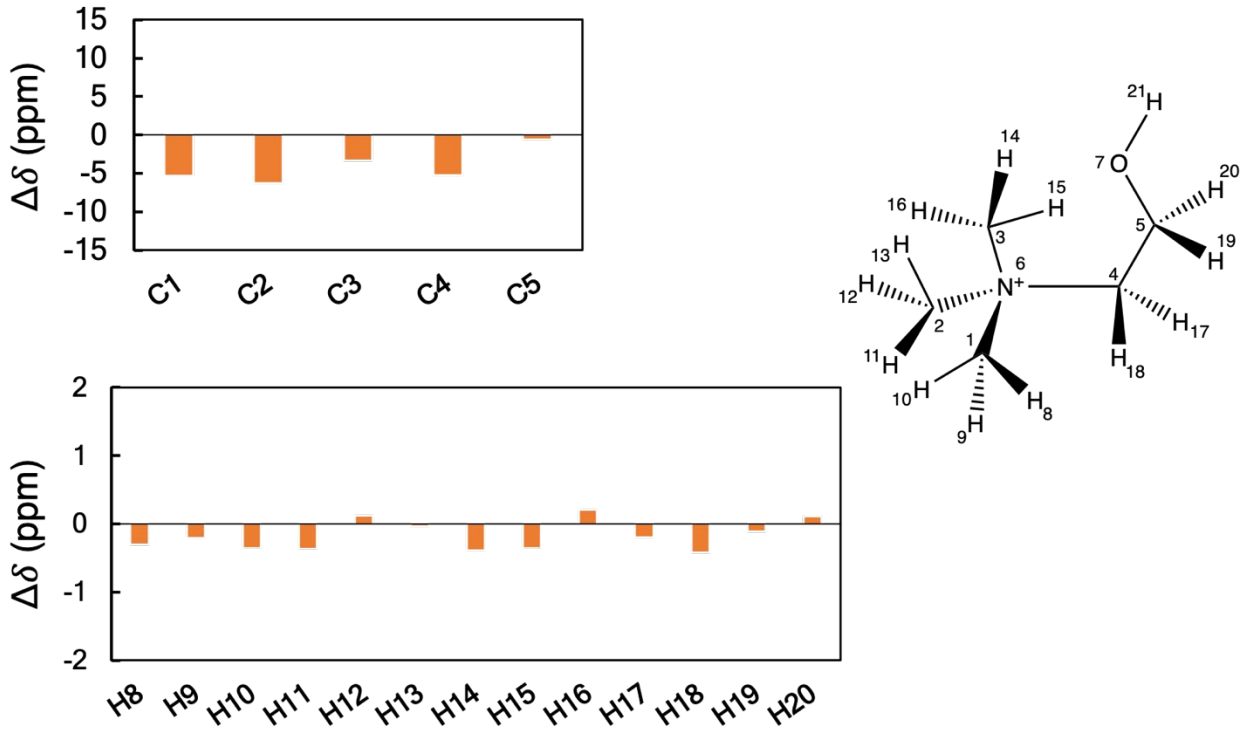

Figure S9. Plots of the differences between the calculated and experimental ^{1}H and ^{13}C NMR chemical shifts of Choline. Shielding constants were computed at the B3LYP/6311G+(2d, p) level of theory and converted to linear scaled reference chemical shifts. Values of chemical shift differences are given in ppm.

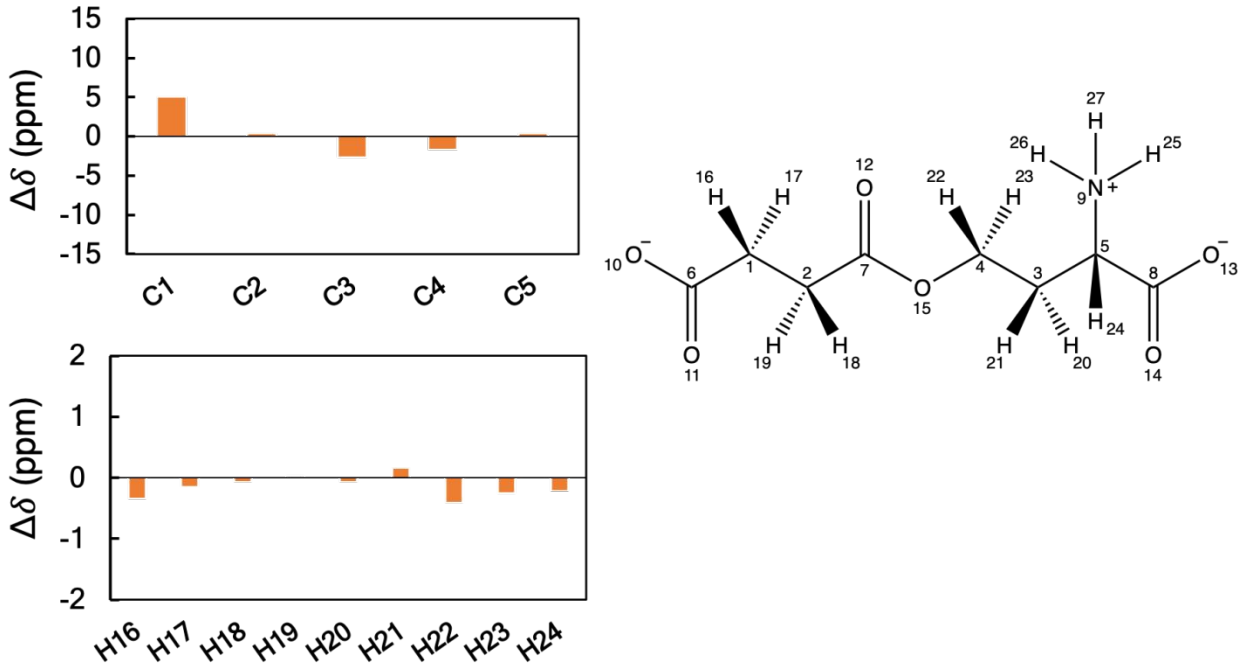

Figure S 10. Plots of the differences between the calculated and experimental ^{1}H and ^{13}C NMR chemical shifts of O-succinyl-L-homoserine (zwitterionic form in the solvent, D_2O). Shielding constants were computed at the B3LYP/6311G+(2d, p) level of theory and converted to linear scaled reference chemical shifts. Values of chemical shift differences are given in ppm.

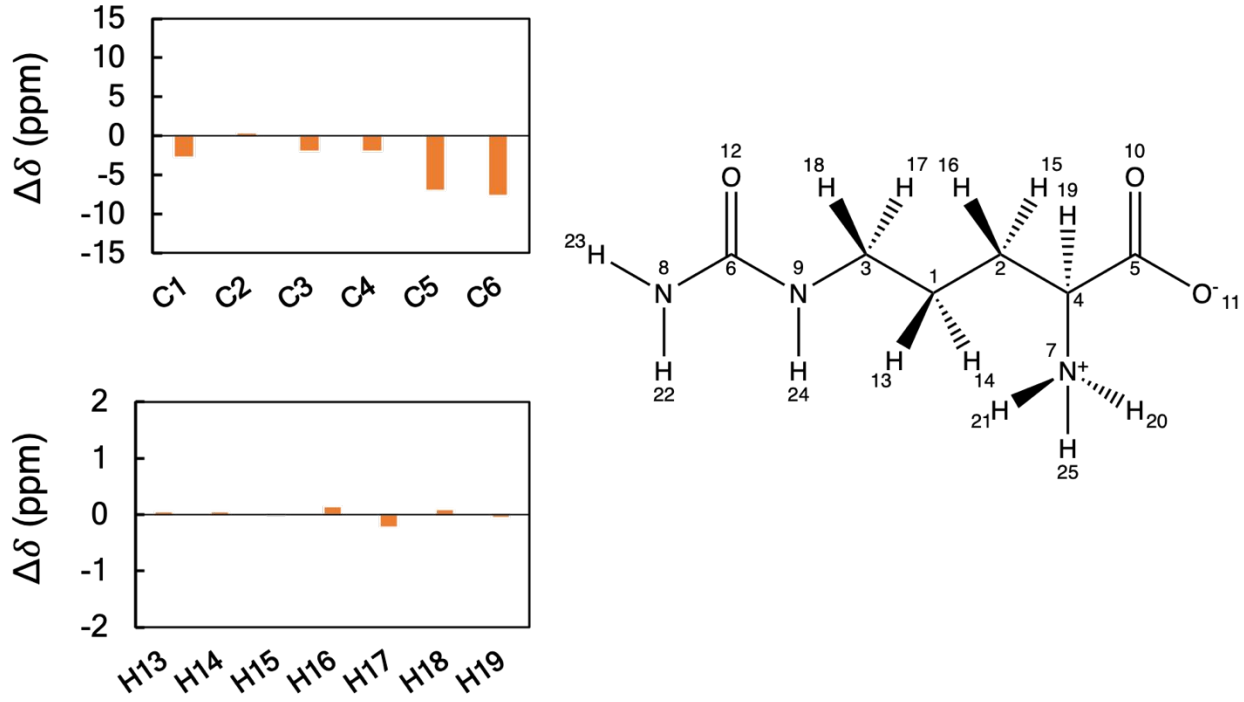

Figure S 11. Plots of the differences between the calculated and experimental ^{1}H and ^{13}C NMR chemical shifts of L-citrulline (zwitterionic form). Shielding constants were computed at the B3LYP/6311G+(2d, p) level of theory and converted to linear scaled reference chemical shifts. Values of chemical shift differences are given in ppm.

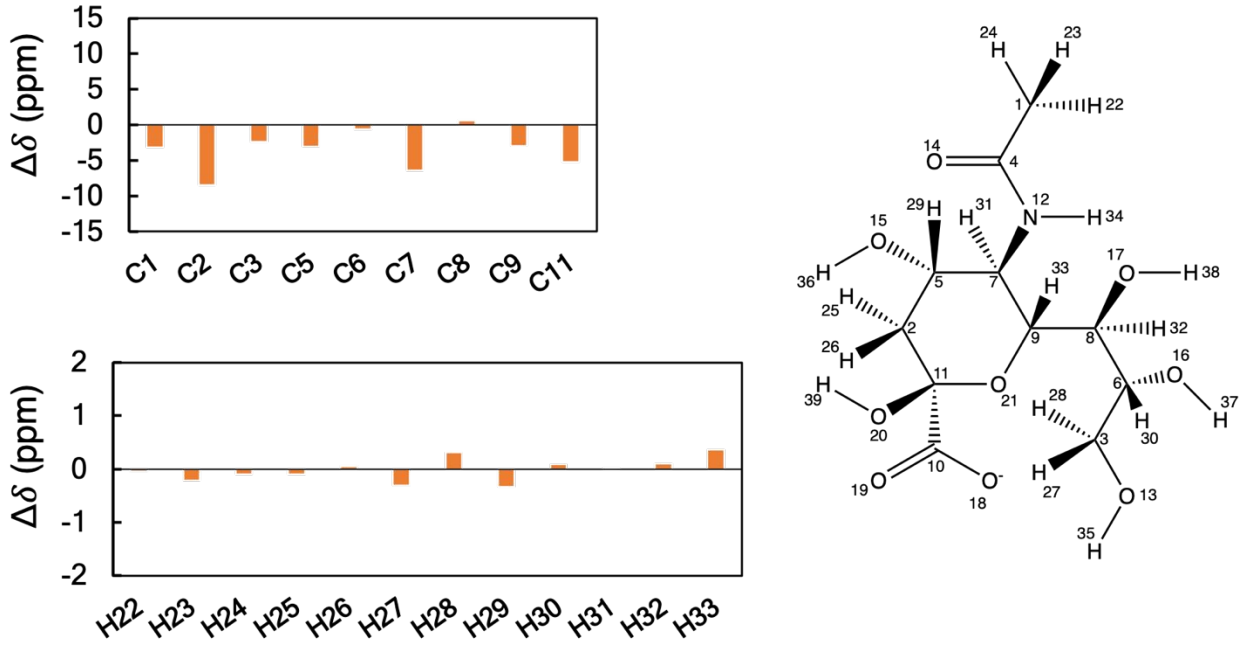

Figure S 12. Plots of the differences between the calculated and experimental ^{1}H and ^{13}C NMR chemical shifts of N-acetylneuraminic-acid (anionic form). Shielding constants were computed at the B3LYP/6311G+(2d, p) level of theory and converted to linear scaled reference chemical shifts. Values of chemical shift differences are given in ppm.

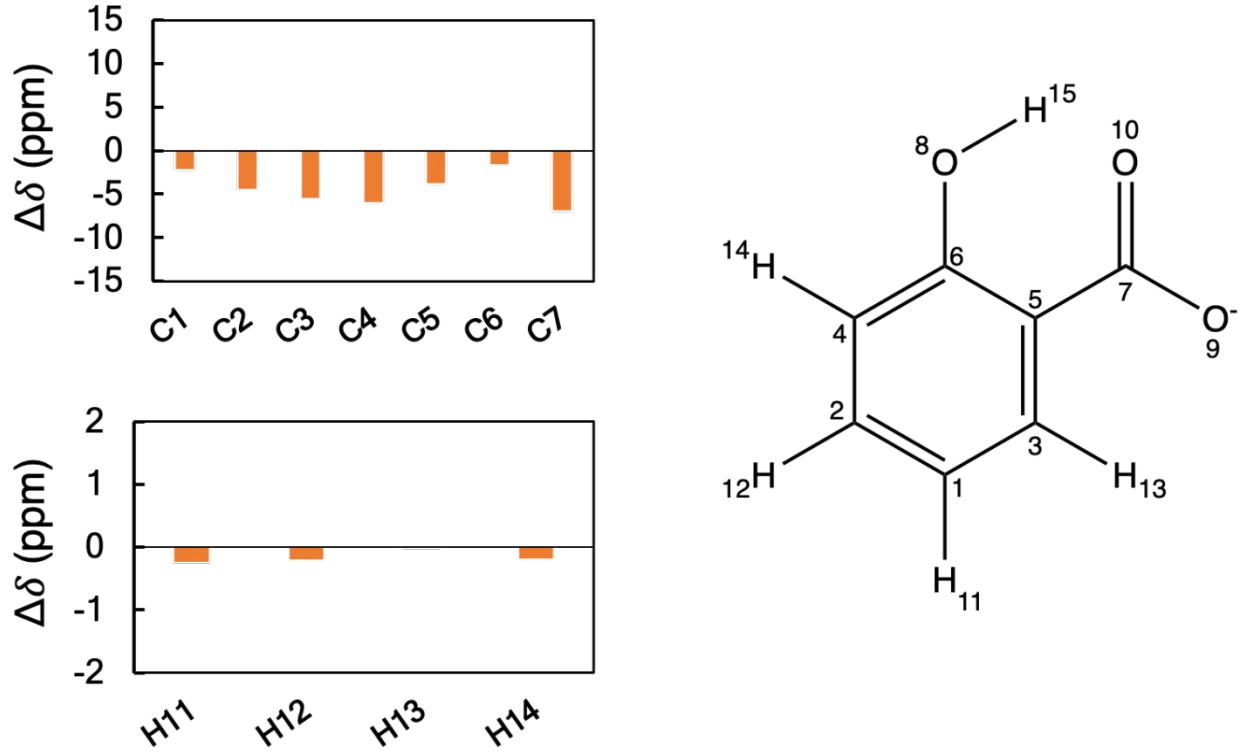

Figure S 13. Plots of the differences between the calculated and experimental ^{1}H and ^{13}C NMR chemical shifts of Salicylate (anionic form). Shielding constants were computed at the B3LYP/6311G+(2d, p) level of theory and converted to linear scaled reference chemical shifts. Values of chemical shift differences are given in ppm.